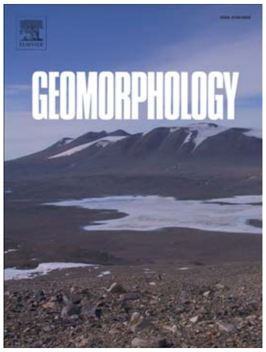

Accepted Manuscript

Subaqueous landslides at the distal basin of Lago Nahuel Huapi (Argentina): Towards a tsunami hazard evaluation in Northern Patagonian lakes

Débora Beigt, Gustavo Villarosa, Eduardo A. Gómez, Carolina Manzoni

PII: S0169-555X(16)30442-1
DOI: doi: 10.1016/j.geomorph.2016.06.004
Reference: GEOMOR 5635

To appear in: *Geomorphology*

Received date: 10 September 2015
Revised date: 2 June 2016
Accepted date: 5 June 2016

SUBAQUEOUS LANDSLIDES AT THE DISTAL BASIN OF LAGO NAHUEL HUAPI (ARGENTINA): TOWARDS A TSUNAMI HAZARD EVALUATION IN NORTHERN PATAGONIAN LAKES

Débora Beigt[1] – Gustavo Villarosa[1,2] – Eduardo A.Gómez[3,4] – Carolina Manzoni[1,2]*

[(1)] Instituto Andino-Patagónico de Tecnologías Biológicas y Geoambientales, UNComa, CONICET, Av. de los Pioneros 2350, (8400) S. C. de Bariloche, Argentina.

[(2)] Universidad Nacional del Comahue, Centro Regional Universitario Bariloche, Quintral 1250, (8400) S.C. de Bariloche, Argentina.

[(3)] Instituto Argentino de Oceanografía, UNS, CONICET, La Carrindanga km 7000, (8000) Bahía Blanca, Argentina.

[(4)] Universidad Tecnológica Nacional, F.R. Bahía Blanca, 11 de abril 46, (8000) Bahía Blanca, Argentina.

**Corresponding author* dbeigt@comahue-conicet.gob.ar, dbeigt@gmail.com

ABSTRACT

The May 22nd 1960 Valdivia earthquake, Chile (Mw 9.5) triggered a series of subaqueous mass-wasting processes (debris flows and slides) in Lago Nahuel Huapi

(Argentina), generating a tsunami-like wave that hit the coasts of San Carlos de Bariloche. Aiming to provide a first preliminary insight into tsunami hazards for the lakeshore communities, in this paper we identify and characterize the subaqueous landslides at the populated distal basin of the lake. Swath bathymetric and seismic profiling surveys were carried out and high-resolution digital elevation models were derived from these data to perform a landslide inventory map. A series of morphometrical parameters (including the landslide area, the volume of displaced materials and the runout distance, among others) were estimated upon selected events. The results indicated that landslide activity at the distal basin of Lago Nahuel Huapi has been concentrated in the vicinity of Bariloche (massive landslide triggered by the 1960 earthquake) and within steep delta fronts where the slope failures typically initiate at shallow waters (9 – 11m depth). The sliding mass frequently travels basinward along a great distance (≥1000m). At the delta fronts, the volume of material removed by landslides can reach ~40 x 10^4 m^3, leaving scar areas of up to 13 m thick. The periodic occurrence of rotational-translational mass movements initiating at the upper edge of the delta fronts, with vertical displacements of the mobilized materials reaching ~200 m, probably represents a potential tsunami hazard for the nearby populated coasts.

Keywords: Lago Nahuel Huapi – subaqueous landslides – lacustrine deltas – tsunami hazard

1. INTRODUCTION

In order to track and understand the various processes shaping the subaqueous environment, high-resolution terrain models generated with modern hydrographic survey tools are the basic form of morphological data (Hilbe et al., 2011). High resolution bathymetry, seismic profiling and sediment coring have allowed the recognition of mass wasting features in the sedimentary infill of several lakes from the Southern Cone of South America (Chapron et al., 2006; Moernaut et al., 2007, 2009, 2014; Volland et al., 2007; Bertrand et al., 2008; Villarosa et al., 2009; Waldmann et al., 2011; Van Daele et al., 2015). Based on the seismic record of Lago Calafquén (Chile), Volland et al. (2007) distinguished 4 different types of mass movement deposits, probably triggered by volcano-tectonic activities at the Chilean active continental margin: slump, mass-flow, debris flow and turbidite deposits. Bertrand et al. (2008) recognized four types of seismically-induced deposits in the Holocene sedimentary infill of Lago Icalma (Chile): slump deposits, chaotic deposits, turbidites and homogenites. Seismic profiling allowed Moernaut et al. (2009) to identify paleoseismic events in Lago Villarica (Chile), which were evidenced by mass-wasting deposits and/or fluidization features. Waldmann et al. (2011) studied a sequence of Holocene mass-wasting events in Lago Fagnano (Argentina), identifying more than 19 mass-flow deposits at the basin floor, interpreted as a result of simultaneously triggered, basin-wide lateral slope failure and the formation of multiple debris flows during paleo-seismic activities along the Magallanes-Fagnano transform fault that runs along the entire lake basin. Chapron et al. (2006) studied the impacts of the 1960 subduction earthquakes and Cordón Caulle eruption in Northern Patagonia, which induced a major hyperpycnal flood deposit in Lago Puyehue (Chile) and a large subaqueous slide and the associated tsunami wave in Lago Nahuel Huapi (Villarosa et al., 2009).

The occurrence of subaerial and/or subaqueous mass-wasting events has frequently been linked to the generation of lacustrine tsunamis (Plafker and Eyzaguirre, 1979; Schnellmann et al., 2002, 2006; Hermanns et al., 2004; Girardclos et al., 2007; Villarosa et al., 2009; Watt et al., 2009; Dirksen et al., 2011; Strasser et al., 2011; Kremer et al., 2012;

Roberts et al., 2013; Lindhorst et al., 2014). The morphometric analysis of subaqueous landslides is therefore a useful tool that provides insight into tsunami hazards (McAdoo and Watts, 2004) for the lakeshore communities. The type of the subaqueous mass failure, the vertical displacement of the mobilized materials, the depth of the mass-movement (Grilli and Watts, 2005 and references therein) and the volume of the slide (Murty, 2003; Fleming et al., 2005) have all been recognized, among others, as parameters governing tsunami amplitudes. Moreover, the location of the mass failure is an important factor to take into account when evaluating tsunami hazard. Run-up on the shore can be significantly higher next to slope failures (Hilbe, 2013), since landslide-induced tsunamis are characterized by locally high amplitudes and run-up relative to the overall run-up distribution (Okal and Synolakis, 2004; Mohammed and Fritz, 2012).

1.1 Study area

Lago Nahuel Huapi (41º01´34´´S, 71º28´38´´W, 764 masl) is a large (~560 km^2) proglacial lake located at the eastern side of the Cordillera de los Andes (Argentina) (Fig. 1). Consisting of seven branches and a distal basin, the lake fills deep glacial valleys shaped during the last Patagonian glaciation (Late Pleistocene), when more than 1000 m-thick glaciers covered Northern Patagonia (Chapron et al., 2006). Glacial erosion produced a characteristic U-shaped lacustrine basin with steep coastal slopes and a flat and deep central area (maximum depth ~464 m).

This region is affected by volcanic and seismic processes generated at the active continental margin in the eastern South Pacific Ocean (Fig. 1). The Instituto Nacional de Prevención Sísmica (Argentinean National Institute of Seismic Prevention, INPRES) considers the Andean portion of Northern Patagonia as a “moderate seismicity” region (INPRES, 1991). The area is also exposed to recurrent ash fall events produced by explosive eruptions from several of the more than 60 active volcanoes present in the Southern Volcanic Zone (Stern, 2004). Volcanic plumes from the active volcanic arc are transported to the east by the dominant Patagonian Westerlies. Thus, the sedimentary infill of Lago Nahuel Huapi is characterized by the presence of abundant glacigenic, fluvial and pyroclastic materials, which where deposited during the deglaciation and throughout the Holocene (Villarosa et al., 2009).

In 1960, the Nazca-South America convergent boundary produced the strongest earthquake ever recorded by instruments (Kanamori, 1977), i.e. the major subduction event (Mw 9.5) of the 21-22 May 1960 Valdivia earthquakes. On May 22, a series of subaqueous mass-wasting processes (including debris flows and slides) triggered by the seismic shock took place at the distal basin of Lago Nahuel Huapi, covering a large area of the lake floor in front of Puerto San Carlos, Bariloche (Villarosa et al., 2009) (Fig. 1). Debris flows developed as a result of the mobilization of sediments in the area where the old pier was settled, probably caused the collapse of the pier. The significant volume of sediments displaced by this massive landslide, which occurred below 70 m depth, generated a tsunami-like wave that hit the coasts of the city (Villarosa et al., 2009). This event, historically documented by detailed reports and photographs offshore Puerto San Carlos (Barros, 1961; Parsons, 2002), caused two fatalities.

Further indication of possible subaqueous mass movements resulted from several low-frequency oscillations in the lake level recently reported by Civil Protection authorities from the coastal city of Villa La Angostura (Fig. 1). These oscillations can be associated with concomitant regional seismicity (e.g. on May 2008, during seismic activity in the Cordón

Caulle volcanic complex; on February 27, 2010 simultaneously to a Mw 8.8 tectonic earthquake with epicenter offshore Bio-Bio (105 km NNE of Concepción, Chile); on July 11, 2011 with intense seismic and volcanic activity recorded during the Cordón Caulle eruption). In any of these cases, there wasn´t any evidence of subaerial mass movements affecting the lake, so the possible mechanisms that could generate these waves are (1) the occurrence of subaqueous landslides triggered by the seismic shaking, which probably induced tsunami-like waves, (2) possible neotectonic activities along faults in the lake floor, or (3) the generation of seiche waves by seismic motion. In order to investigate the 1st and 2nd hypotheses, the morphology and stratigraphy of the lake floor have been surveyed in the last years, looking for evidence of mass-wasting and/or possible fault displacements.

The first study at this line of research in Lago Nahuel Huapi was conducted by Villarosa et al. (2009), who investigated the mechanisms that originated the 1960 tsunami in the distal basin. Through high resolution bathymetry, seismic profiling and sediment coring, they could establish a link between the 1960 Valdivia earthquake and a massive landslide initiated at the lake floor, in front of Puerto San Carlos. Another study performed on the lacustrine deltas of Pireco and Totoral streams (located about 11 km westwards from Villa La Angostura and ~30 km from the Puyehue-Cordón Caulle volcanic complex), where the slope of the delta fronts range between 14° and 22°, allowed the identification of several landslides and channelized debris flows(?) initiated at the delta fronts (Beigt et al., 2012a). Furthermore, increasing sedimentation rates and deltaic plain progradation registered at these deltas during the recent ash fall event produced by the 2011/12 Cordón Caulle eruption (Beigt et al., 2012b) suggest that these recurrent events could periodically lead to instability at these deltas located at proximal volcanic areas, where the occurrence of large subaqueous landslides could certainly represent a potential tsunami hazard for nearby populated coasts of Villa La Angostura. Beigt et al. (2014a) carried out a first preliminary study about the subaqueous morphology at Ñirihuau and Ñireco deltas (Fig. 1). They found three depositional environments at these deltas: a subaerial deltaic plain, a steep delta front where sediments are mobilized by gravitational processes, and a gently-inclined prodelta. Storm waves seem to substantially modify the subaquatic morphology of these deltas during periods of low water level by generating an abrasional platform (up to 150 m wide) located between the subaerial plain and the deltaic front.

Through a landslide inventory and morphometric analysis of the subaqueous slope failures at the coastal areas of the populated distal basin of Lago Nahuel Huapi (where the 1960 earthquake-induced subaqueous slide and the associated tsunami wave took place), this study aims to improve our knowledge about the geological hazards affecting the lakeshore communities, serving as a preliminary step towards a tsunami hazard evaluation. It is worth mentioning that the coastal cities of the distal basin (S. C. de Bariloche and Dina Huapi) have registered rapid population growth within the last decades. This has led to an intense occupation of the coastal areas, including particularly active environments such as deltaic plains. Tourism, the main industry in both cities, also played an important role in the coastal urban expansion, which in turn has considerably increased the vulnerability of the lakeshore communities to landslide-induced tsunamis.

2. METHODS

Bathymetric survey was carried out on April 2010 and November 2011 using a Phase Measuring Bathymetric Sonar System ("GeoSwath Plus Bathymetry System", GeoAcoustic Ltd.) (IADO-CONICET) that emulates the perfomance of multibeam systems for shallow water depths (Gómez and Maraschin, 2006). The system was equipped with

250 kHz transducers, allowing high-resolution data of the bed morphology up to its maximum operating water depth (100-120 m). It was mounted onboard a vessel from Prefectura Naval Argentina (the national coastguard). Sound velocity profiles were registered using a Midas SVP (Valeport Ltd.). A ground-based reference station was established for the differential GPS. Tracks were covered following an approximately parallel direction to the coastline, with a 50-percent overlap between adjacent swaths. A sub-bottom profiler (StrataBox 3510^{TM}, SyQwest) (IADO-CONICET) equipped with 3.5 kHz transducers was used to perform a seismic survey on the lake floor on May and October 2014.

The stratigraphic characteristics of mobilized and undisturbed areas of the lake bed were analyzed using the StrataBox software. Digital elevation models, shaded-relief, aspect and slope maps, bathymetric maps and profiles were derived from the bathymetric data using Surfer v8 and ArcGIS v8.1. The areas affected by mass failure were outlined and a landslide inventory map was performed (Fig. 2). Based on previous work on numerical modelling of landslide-generated tsunamis (McAdoo and Watts, 2004; Fine et al., 2005; Lovholt et al., 2005; Zaniboni et al., 2014), a series of morphometric parameters was selected for this study (Table 1). The morphometric analysis was performed upon six landslides (Fig. 2), including (1) the largest events (Niri1, Niri2, Nire1 and Nire2) identified in the subaqueous portion of Ñireco and Ñirihuau deltas, (2) the main single landslide registered on the coasts of Bariloche (Bar1), and (3) the largest event identified in the Castilla delta (Cas1), located at the northern coast. Numerous transverse and longitudinal bathymetric profiles across these landslides were used to estimate the height and slope of the scarps, the slope of the failure planes and the slope of the unmobilized adjacent areas. Following the methods applied by ten Brink et al. (2006) and Chaytor et al. (2007), the volume of materials displaced by each landslide event was calculated by interpolating a smooth surface (as a representation of the floor prior to the slope failure) through a polygon that defines the edges of the slide, gridding this smooth surface, and subtracting this grid from the gridded topography of the landslide source excavation areas. The grid size for both the topography and the smoothed surface was 3 m. Natural Neighbour interpolation was applied. Subtracting the original ground surface (interpolated grid) from the post-landslide surface also allowed the identification of the depletion and accumulation zones (Xue et al., 2014).

3. RESULTS

An overview of the landslide inventory (Fig. 2) shows the coastal environments prone to subaqueous landsliding at the distal basin. A total of 40 landslides (~20 landslides in each delta) have been identified at Ñirihuau and Nireco deltas, covering extensive areas of ~2.6 x 10^6 m^2 and ~9.9 x 10^5 m^2 in each delta, respectively. The mobilized area at the coasts of Bariloche city covers ~7.6 x 10^5 m^2. A small number of these processes were identified in deltaic environments from Castilla (11 events) and Gutiérrez (1 event) streams, while some other landslides were found to the east of the studied deltas (Fig. 2).

The headwalls of non-deltaic subaqueous landslides are generally located below a water depth of ~50 m. The largest single event (Bar1, Fig. 3) occurred at a water depth of 64 m, cutting across massive sediments (Fig. 4) that could have been deposited by a previous mass-movement upslope. The bathymetric survey over Bar1 covered a mobilized area of ~29 x 10^3 m^2 belonging to its depletion zone, with a maximum scar thickness of ~6 m (Fig. 3). This event was interpreted as a translational slide that probably evolved into a mass flow, involving a mass waste deposit at the deep basin (Fig. 4), ~1000 m from the landslide headscarp. It is noteworthy that the failure initiated at a steep slope that is coincident with a structural lineament identified in the lake floor (Figs. 3, 4), where morphology and seismic data suggest the presence of a fault that affects the basement rocks.

On the other hand, deltaic slope failures occur at shallow waters (9 – 11 m depth). The larger individual failures (considering both landslide area and volume) were identified at Ñireco and Ñirihuau´ deltas (Table 1). The materials removed by Nire2 and Niri2 reached ~40 x 10^4 m^3, leaving a deep scar area of up to 13 m thick at both landslides (Figs. 5, 6). On the other hand, Cas1 involved a small area and volume, with a maximum scar thickness of ~6 m. The materials were mobilized along a steep slope (slope gradient of the slip surface=24°) and were accumulated at a depth of 60 m and more (Fig. 3).

Nire2 initiated at the frontal crest, cutting across a massive alluvium deposited at the proximal deltaic environment (Fig. 7). The displaced materials travelled a distance of approximately 730 m along the delta slope towards a depth of 130-170 m, where a coherent mass was deposited. A group of positive forms, indicating mass deposits, are located immediately below this depth at the transitional area between the delta face and prodelta. Horizontally-stratified materials at the prodelta are interpreted as undisturbed basin sediments. A mass-wasting deposit resulting from Nire2 failure is located on top of these sediments, ~1700 m from the landslide headscarp. Overlying the landslide features at the proximal deltaic environment, a reflective layer of stratified material probably represents the tephra from the Cordón Caulle eruption (initiated in June 2011) (Fig. 7A). This tephra layer overlies undisturbed (U) as well as mobilized areas (Fig. 7B).

The topography of the landslides scars and deposits at Ñireco and Ñirihuau deltas was strongly modified by localized mass-movements (rotational slides?) as well as channelized debris flows (Figs. 5, 6, 7B) that probably operated during the downslope transport of the landslide materials and/or were generated later on. A series of sediment waves located at both deltas at depths exceeding 40 m probably indicate the presence of turbidity or bottom currents. These bedforms are located at a depth range between 85 m and 130 m at Nire2 (Fig. 7A). The areas affected by these processes are mainly coincident with depletion areas (Figs. 5, 6) within the landslide accumulation zones, indicating that post-landslide currents reworked these mass waste deposits by tractional mechanisms.

The slipped materials at Ñireco and Ñirihuau´deltas typically begin to accumulate at depths of 50 m and deeper, at a distance of about 150 m to 350 m from the headscarps (Figs. 5, 6). Nire1 exhibits the greatest accumulation volume within the surveyed area, involving about 50 % of the removed materials (Table 1). These deposits are up to 4 m-thick and cover an area of 57 x 10^3 m^2 (42 % of the total landslide area). On the other hand, Niri1 deposits are absent in the surveyed area despite the gentle slope of the slip surface (Table 1). A probable explanation for this depletion is the transformation of the slope failure into a debris flow that transported the displaced materials towards deeper areas of the lacustrine basin. This hypothesis is supported by the presence of a 45 m-wide and 2 m-deep subaqueous channel in the lower part of the landslide (Fig 5).

4. DISCUSSION

Several bathymetric surveys performed along different littoral environments in Lago Nahuel Huapi (Beigt et al., 2010, 2012a,b, 2014a,b, this work) show that subaqueous mass wasting activity in this lake has been concentrated (1) at the coasts of Bariloche city (this area was affected by a massive landslide triggered by the 1960 earthquake, Villarosa et al., 2009) and (2) throughout the deltaic fronts of lacustrine deltas. In particular, the steep deltaic fronts (14°-17° slopes, Beigt et al., 2014a) from Ñireco and Ñirihuau deltas show the vast majority of the deltaic slope failures identified at the distal basin (Fig. 2).

Non-deltaic subaqueous landslides occur at a depth of 50 m and more. The particular location of Bar1 headscarp suggests that the occurrence of this slide could have been influenced by the presence of the structural lineament described in the results. The available seismic data suggests possible neotectonic activity that affected the postglacial deposits. These studies are still in progress and their results will be discussed in a future work, along with some considerations about its potential implications in lacustrine tsunami generation.

On the other hand, deltaic slope failures initiate at the upper edge of the delta fronts, at a shallow depth of 9–11 m (Beigt et al., 2014a). Mass-movements generated right below the brink point (frontal crest) are expected on a steep delta face, where the transport of alluvial sediments over the delta brink creates a continuous influx of particles to the subaqueous delta slope, resulting in the steepening of the subaqueous slope (Nemec, 1990).

Subaqueous landsliding at the coastal zone and subsequent mass flows and turbidity currents play an important role in the sedimentation of the distal basin by periodically transporting sediments mainly from the delta fronts (i.e. fluvial and pyroclastic materials) towards the deep basin. Mass flows resulting from subaqueous slides at the distal basin of Lago Nahuel Huapi have already been mentioned by Chapron et al. (2006) and Villarosa et al. (2009), who found evidence of a megaturbidite at ~200 m depth in the deep basin. This deposit was linked to the subaqueous mass-movement triggered by the 1960 Valdivia earthquake, indicating that the materials displaced by this massive landslide were transported by turbidity currents over a distance of about 3000 m towards the flat and deep central area.

The results of the present work showed that the sliding mass frequently travels basinward along a great distance (≥1000 m). The vast majority of the deltaic mass-movements - including the ones selected for this study (Figs. 3, 5, 6) - show arcuate-shaped crowns and a headscarp concave profile, suggesting that rotational mass movement is the dominant failure mechanism at these environments. However, the presence of long sidewalls extending beyond the area of the bathymetric survey (which covered a coastal strip ~300 m, ~600 m and ~1000 m wide in Castilla, Ñireco and Ñirihuau deltas, respectively) suggests that these rotational slides could have evolved into translational slides. The estimated volume of deltaic landslide deposits throughout this area is notably smaller (differing by one order of magnitude) compared to the volume removed (Table 1), indicating that most of these materials where displaced towards deeper areas of the lacustrine basin.

A series of gravitational processes such as rotational slides and debris flows (generated at the delta fronts during the displacement of the landslide materials, or later on) indicate once again that the delta fronts are highly dynamic, where a common reworking of the landslide scars and deposits take place. Reworking of the mass wasting deposits is also produced by bottom or turbidity currents, which is evidenced by the presence of a series of sediment waves at depths exceeding 40 m at Ñireco and Ñirihuau deltas. Similar morphologies have been studied by Gilbert and Crookshanks (2009), Turmel et al. (2010), Cartigny et al. (2011) and Moore et al. (2014), who attributed these bedforms to the action of turbidity currents. These features and their possible origin are being studied and will be discussed in detail in future work. On the other hand, landslides found to the east of the studied deltas (Fig. 2) could be related to transport and deposition of deltaic sediments by long-shore currents driven by the strong, constant Southern Hemisphere Westerlies that prevail in the Patagonian Region (Paruelo et al., 1998; Garreaud, 2009). Uniform wind stress has been commonly cited as responsible for long-shore, downwind currents in the coastal areas of a lake (Bennett, 1974; Beletsky et al., 2003). Rapid deposition and high slopes of the resulting deposits could act as preconditioning factors, increasing instability at these areas.

Whereas Gutiérrez is the outlet stream from Gutiérrez lake (750 masl), Ñireco and Ñirihuau headwaters are in the Andean range at ~2000 masl (Fig. 1), resulting in topographic gradients of about 1300 m along their drainage basins. These gradients, together with their high discharge, imply higher sediment loads at these streams. On the other hand, the relatively small basins of Gutierrez and Castilla streams and the presence of a lake in the head of Gutierrez basin significantly reduce the volume of materials to be deposited at these deltas. The major portion of the sediment load transported by Gutiérrez stream is supplied by its affluent (La Cascada stream), which descends the northeastern flank of Cerro Catedral (Fig. 1) from its headwaters located at ~1700 masl. All these factors control the sediment characteristics and dynamics at the subaqueous portion of each delta (especially sedimentation rates and density current occurrence), increasing instability at Ñireco and Ñirihuau delta fronts, where a higher landslide abundance was identified. Larger mass-wasting morphological features (considering both landslide area and volume) identified at Ñirihuau and Ñireco deltas (Table 1) could be linked to higher sedimentation rates. This observation leads us to propose that triggering factors over sedimentation rates are the main controlling variable for the occurrence of mass-wasting processes in these environments. This suggests relatively similar mass-wasting frequencies related to regional seismic recurrence intervals in deltaic environments;

therefore explaining the higher dimensions of the resulting geomorphic features. These urbanized deltas are located at the coasts of Bariloche and Dina Huapi cities, respectively. The periodic occurrence of rotational-translational mass movements initiating in shallow waters (involving up to ~40 x 10^4 m^3 of removed materials), with vertical displacements of the mobilized materials reaching ~200 m, probably represents a potential tsunami hazard. Particularly, these mass-movements could create strong local effects at the nearby populated coasts. The effects could be amplified during a strong earthquake, when the probability of occurrence of large landslides at the distal basin would increase.

The recurrent character of slope failures at the distal basin of Lago Nahuel Huapi, evidenced in the seismic profiles by recent and older mass wasting deposits (Chapron et al., 2006; Villarosa et al., 2009, this article), calls attention to the possible occurrence of future events affecting vulnerable coasts. Preconditioning factors of subaqueous landsliding in non-deltaic coastal environments probably include (1) anthropogenic activities at subaerial/subaqueous slopes (the 1960 events leading to the tsunami wave were probably favoured by the prolonged vibrations exerted during the reconstruction of the pier, 1958-1960), (2) steep coastal slopes of the lacustrine basin and (3) the presence of non-cohesive tephra layers, which could serve as detachment surfaces (Harders et al., 2010). Furthermore, it is well-known that active river deltas are subject to widespread subaqueous landsliding on the continental margin (Hampton et al., 1996) as well as in lakes (Girardclos et al., 2007; Beck, 2009; Wirth et al., 2011; Kremer et al., 2012, among others) due to (1) the rapid accumulations of thick sedimentary deposits and (2) the presence of sloping delta fronts. The slope gradients of Ñirihuau and Ñireco delta fronts, which range from 14° to 17° (Beigt et al., 2014a), fall into the range cited in the literature for Gilbert-type delta fronts (10-25°, Postma and Roep, 1985), where mass-failure is a common phenomenon. On the other hand, the ash fall produced by the explosive eruptions of the Andean volcanoes recurrently affects the watersheds located at proximal and medial volcanic areas, modifying the sedimentary dynamics of their deltas. The input of pyroclastic materials transported by these streams towards their deltas causes a rapid progradation of the deltaic plains (Beigt et al., 2012*b*). The presence of thick deposits of non-cohesive, liquefaction-prone(?) pyroclastic materials at the delta fronts could cause instability in these environments, serving as potential failure planes in the lacustrine basin.

5. CONCLUSIONS

The 1960 tsunami in Lago Nahuel Huapi, as well as recently reported low-frequency oscillations in the lake level –which are concomitant to regional earthquakes- are clear indications of tsunamigenic activities in the lacustrine basin. Through morphometric analysis of the subaqueous slope failures in coastal areas of the distal basin, this study has improved our knowledge about the natural hazards affecting the lakeshore communities, serving as a preliminary step towards a tsunami hazard evaluation. The results highlighted lacustrine deltas and their surroundings as one of the most landslide-prone areas of the distal basin, along with the populated coasts of Bariloche city, where the 1960 landslide and the associated tsunami wave were generated. The periodic occurrence of rotational-translational mass movements at the subaqueous portion of urbanized deltas could certainly represent a potential tsunami hazard for the nearby Bariloche and Dina Huapi cities due to the volume of the removed materials (involving up to ~40 x 10^4 m^3), their vertical displacement (reaching ~200 m) and the shallow depths where the failures initiate (9-11 m).

Subaqueous landsliding is thus a common process in the study area. Together with subsequent mass flows and turbidity currents, landslides play an important role in the sedimentation of the lacustrine basin by periodically transporting sediments mainly from the delta fronts towards the flat and deep basin. Currents (turbidity or bottom currents, long-shore currents) seem to play an important role shaping the subaqueous topography of the delta fronts, prodeltas and their surroundings. This is an important issue to deal with in future studies in order to improve our knowledge about the sediment dynamics in deltaic environments. On the other hand, the presence of a structural lineament at the southern shore of Lago Nahuel Huapi arises a new question regarding a potential fault displacement at the subaqueous environment as another possible mechanism of tsunami generation. The investigation about possible neotectonic features in the lake is still in progress and will be discussed in future work.

6. ACKNOWLEDGEMENTS

This study was funded by the Agencia Nacional de Promoción Científica y Tecnológica (PICT 2010-0636, PICT 2010-2046), the Ministerio de Ciencia, Tecnología e Innovación Productiva (PROEVO 40-B-187, PROEVO 40-B-188), the Universidad Tecnológica Nacional (PID 25/B035-UTI989) and the Universidad Nacional del Comahue (PIN I B 191). The authors wish to thank Prefectura Naval Argentina (San Carlos de Bariloche) for the logistics support during field work.

7. REFERENCES

Barros, G., 1961. El maremoto del 22 de mayo de 1960 en las costas de Chile, Departamento de Navegación e Hidrografía de la Armada de Chile, Santiago.

Beck, C., 2009. Late Quaternary lacustrine paleo-seismic archives in north-western Alps: Examples of earthquake-origin assessment of sedimentary disturbances. Earth-Science Reviews 96, 327 – 344.

Beigt, D., Villarosa, G., Gómez, E. A., 2010. Mass-wasting events and related morphology along a coastal portion of Nahuel Huapi lake bed (Patagonia). 18th International Sedimentological Congress. IAS. Mendoza. pp.166.

Beigt, D., Villarosa, G., Gómez, E.A., 2012*a*. Deslizamientos subacuáticos en sistemas deltaicos del lago Nahuel Huapi: resultados preliminares de una evaluación de peligrosidad para la localidad de Villa La Angostura (Neuquén). 2das Jornadas Nacionales de Investigación y Docencia en Geografía Argentina (2da. JONIDGA) y 8vas. Jornadas de Investigación y Extensión del Centro de Investigaciones Geográficas (8° JIECIG). Centro de Investigaciones Geográficas y Universidad Nacional del Centro. Tandil. pp. 1-7.

Beigt, D., Villarosa, G., Outes, V., Dzendoletas, M.A., Gómez, E. A., 2012*b*. El lago Nahuel Huapi: un registro de erupciones, deslizamientos y tsunamis. Ciencia Hoy 22 (130), 50 – 56.

Beigt, D., Villarosa, G., Gómez, E. A., 2014a. Análisis de deslizamientos subacuáticos en deltas lacustres (lago Nahuel Huapi, Argentina) a partir de batimetrías de alta resolución. Cuadernos de Investigación Geográfica 40 (1), 247 – 259.

Beigt, D., Manzoni, C., Villarosa, G., Gómez, E.A., 2014b. Estudio de los deslizamientos subacuáticos en la cuenca distal del lago Nahuel Huapi (Argentina) a partir de batimetrías de alta resolución. XIX Congreso Geológico Argentino. Asociación Geológica Argentina. Córdoba, pp. 1300-1301.

Beletsky, D., Schwab, D. J., Roebber, P. J., McCormick, M. J., Miller, G. S., Saylor, J. H., 2003. Modeling wind-driven circulation during the March 1998 sediment resuspension event in Lake Michigan. Journal of Geophysical Research 108 (C2), 3038 doi:10.1029/2001JC001159.

Bennett, J. R., 1974. On the dynamics of wind-driven lake currents. Journal of Physical Oceanography 4, 400 – 414.

Bertrand, S., Charlet, F., Chapron, E., Fagel, N., De Batist, M., 2008. Reconstruction of the Holocene seismotectonic activity of the Southern Andes from seismites recorded in Lago Icalma, Chile, 39°S. Palaeogeography, Palaeoclimatology, Palaeoecology 259, 301 – 322.

Cartigny, M.J.B., Postma, G., van den Berg, J.H., Mastbergen, D.R., 2011. A comparative study of sediment waves and cyclic steps based on geometries, internal structures and numerical modeling. Marine Geology 280, 40 – 56.

Chapron, E., Ariztegui, D., Mulsow, S., Villarosa, G., Pino, M., Outes, V., Juvignie, Etienne, Crivelli, E., 2006. Impact of the 1960 major subduction earthquake in Northern Patagonia (Chile, Argentina). Quaternary International 158, 58 – 71.

Chaytor, J.D., Twichell, D.C., Ten Brink, U.S., Buczkowski, B.J., Andrews, B.D., 2007.

Revisiting submarine mass movements along the U.S. Atlantic Continental Margin: Implications for tsunami hazards. In: Lykousis. V., Sakellariou, D. and Locat, J. (eds.). Submarine Mass Movements and Their Consequences. Advances in Natural and Technological Hazards Research. Springer Netherlands, Netherlands, pp.395-403.

Dirksen, O., van den Bogaard, C., Tohru, D. and Diekmann, B.,2011. Tephrochronological investigation at Dvuh-yurtochnoe lake area, Kamchatka: Numerous landslides and lake tsunami, and their environmental impacts. Quaternary International 246, 298-311.

Fine, I.V., Rabinovich, A.B., Bornhold, B.D., Thomson, R.E., Kulikov, E.A., 2005. The Grand Banks landslide-generated tsunami of November 18, 1929: preliminary analysis and numerical modeling. Marine Geology 215, 45 – 57.

Fleming, J.G., Walters, R.A., Sue, L.P., Nokes, R.I., 2005. Experimental design for solid block and granular submarine landslides: a unified approach. In: Satake, K. (ed.), Tsunamis: Case Studies and Recent Developments. Advances in Natural and Technological Hazards Research. Springer Netherlands, Netherlands, pp. 259-279.

Garreaud, R.D., 2009. The Andes climate and weather. Advances in Geosciences 22, 3 – 11.

Gilbert, R., Crookshanks, S., 2009. Sediment waves in a modern high-energy glacilacustrine environment. Sedimentology 56, 645 – 659.

Girardclos, S., Schmidt, O.T., Sturm, M. Ariztegui, D., Pugin, A., Anselmetti, F.S.,2007. The 1996 AD delta collapse and large turbidite in Lake Brienz. Marine Geology 241, 137-

154.

Gómez, E. A., Maraschin, S. D., 2006. Sonar Batimétrico por Medición de Fase: nueva herramienta para estudiar la morfología y sedimentología subácuea. IV Congreso Latinoamericano de Sedimentología y XI Reunión Argentina de Sedimentología. Asociación Argentina de Sedimentología. Bariloche, pp. 112.

Grilli, S.T., Watts, P., 2005. Tsunami generation by submarine mass failure.I: Modeling, experimental validation and sensitivity analyses. Journal of Waterway, Port, Coastal and Ocean Engineering ASCE. 283 – 297.

Hampton, M.A., Lee, H.J., Locat, J.,1996. Submarine landslides. Reviews of Geophysics 34 (1), 33 – 59.

Harders, R., Kutterolf, *S.,* Hensen, *C.,* Moerz,*T.,* Bruekmann, W., 2010. Tephra layers: A controlling factor on submarine translational sliding? Geochemistry. Geophysics. Geosystems. 11 (5), 1-18.

Hermanns, R.L., Niedermann, S., Ivy-Ochs, S., Kubik, P.W., 2004. Rock avalanching into a landslide-dammed lake causing multiple dam failure in Las Conchas valley (NW Argentina) – evidence from surface exposure dating and stratigraphic analyses. Landslides 1, 113 – 122.

Hilbe, M., Anselmetti, F.S., Eilertsen, R.S., Hansen, L., Wildi, W., 2011. Subaqueous morphology of Lake Lucerne (Central Switzerland): implications for mass movements and glacial history. Swiss J. Geosci. 104, 425 - 443.

Hilbe, M.J., 2013. Subaqueous morphology and natural hazards in perialpine Lake Lucerne (Central Switzerland). DISS. ETH Nr. 21459. Department of Environmental Sciences, ETH-Zürich.

INPRES, 1991. Reglamento INPRES-CIRSOC 103. Parte I. Normas argentinas para construcciones sismorresistentes. 206.

Kanamori, H., 1977. The energy release in great earthquakes. Journal of Geophysical Research 82, 2981–2987.

Kremer, K., Simpson, G., Girardclos, S., 2012. Giant Lake Geneva tsunami in AD 563. Nature Geoscience 5, 756-757.

Lindhorst, K., Krastel, S., Papenberg, C., Heidarzadeh, M., 2014. Modeling submarine landslide-generated waves in Lake Ohrid, Macedonia/Albania. In: Krastel, S. et al. (eds). Submarine mass-movements and their consequences. Advances in Natural and Technological Hazards Research 37, 497 – 506.

Lovholt, F., Harbitz, C.B., Haugen, K.B., 2005. A parametric study of tsunamis generated by submarine slides in the Ormen Lange/Storegga area off western Norway. Marine and Petroleum Geology 22, 219 – 231.

McAdoo, B.G., Watts, P., 2004. Tsunami hazard from submarine landslides on the Oregon continental slope. Marine Geology 203 (3-4), 235 – 245.

Moernaut, J., De Batist, M., Charlet, F., Heirman, K., Chapron, E., Pino, M., Brummer, R., Urrutia, R., 2007. Giant earthquakes in South-Central Chile revealed by Holocene mass-wasting events in Lake Puyehue. Sedimentary Geology 195 (3–4), 239–256.

Moernaut, J., De Batist, M., Heirman, K., Van Daele, M., Pino, M., Brummer, R., Urrutia, R., 2009. Fluidization of buried mass-wasting deposits in lake sediments and its relevance for paleoseismology: results from a reflection seismic study of lakes Villarrica and Calafquén (South-Central Chile). Sedimentary Geology 213 (3–4), 121–135.

Moernaut, J., Van Daele, M., Heirman, K., Fontijn, K., Strasser.M., Pino, M., Urrutia, R., De Batist, M., 2014. Lacustrine turbidites as a tool for quantitative earthquake reconstruction: New evidence for a variable rupture mode in south central Chile. Journal of Geophysical Research: Solid Earth 119 (3), 1607 – 1633.

Mohammed, F., Fritz, H.M., 2012. Physical modeling of tsunamis generated by three-dimensional deformable granular landslides. Journal of Geophysical Research 117 (C11), 20.

Moore, J.G., Schweickert, R.A., Kitts, C.A., 2014. Tsunami-generated sediment wave channels at Lake Tahoe, California-Nevada, USA. Geosphere 10, 757-768.

Murty, T. S., 2003. Tsunami wave height dependence on landslide volume. Pure and Applied Geophysics 160 (10-11), 2147-2153.

Nemec, W.,1990. Aspects of sediment movement on steep delta slopes. In: Colella, A., Prior, D.B.(eds.). Coarse Grained Deltas: Special Publications of the International

Association of Sedimentologists 10. The International Association of Sedimentologists, Blackwell Scientific Publications, pp. 29-73.

Okal, E.A., Synolakis, C.E., 2004. Source discriminants for near-field tsunamis. Geophys. J. Int. 158, 899 – 912.

Parsons T.W., 2002. Enciclopedia histórica centenaria de Bariloche, 3 de mayo de 1902-3 de mayo de 2002, tomo 1, 150.

Paruelo, J.M., Beltrán, A., Jobbágy, E., Sala, O.E., Golluscio, R.A., 1998. The climate of Patagonia: general patterns and controls on biotic processes. Ecología Austral 8, 85 – 101.

Plafker, G., Eyzaguirre, V. R., 1979. Rock avalanche and wave at Chungar, Perú. In: Voight, B. (Ed.): Rockslides and Avalanches, vol. 2. Developments in Engineering Geology Elsevier, NL. 14B, pp.269-279.

Postma, G., Roep, T.B., 1985. Resedimented conglomerates in the bottomsets of Gilbert-type gravel deltas. Journal of Sedimentary Petrology 55 (6), 874-885.

Roberts, N.J., McKillop, R.J., Lawrence, M.S., Psutka, J.F., Clague, J.J., Brideau, M.A., Ward, B.C., 2013. Impacts of the 2007 landslide-generated tsunami in Chehalis Lake, Canada. In: Margottini, C., Canuti, P., Sassa, K. (eds.). Landslide Science and Practice, Volume 6: Risk Assessment, Management and Mitigation. pp. 133-140.

Schnellmann, M., Anselmetti, F.S., Giardini, D., McKenzie, J.A., Ward, S.N., 2002. Prehistoric earthquake history revealed by lacustrine slump deposits. Geology 30, 1131–1134.

Schnellmann, M., Anselmetti, F.S., McKenzie, J.A., Giardini, D., 2006. 15,000 yr of mass movement history in Lake Lucerne: implications for seismic and tsunami hazards. Eclogae Geol. Helv. 99. doi:10.1007/s00015-006-1196-7.

Stern, C.R., 2004. Active Andean volcanism: its geologic and tectonic setting. Revista Geológica de Chile 31(2), 161-206.

Strasser, M., Hilbe, M., Anselmetti, F., 2011. Mapping basin-wide subaquatic slope failure susceptibility as a tool to asses regional seismic and tsunami hazards. Marine Geophysical Research 32 (1/2), 331 – 347.

ten Brink, U.S., Geist, E.L., Andrews, B.D., 2006. Size distribution of submarine landslides and its implications to tsunami hazard in Puerto Rico. Geophysical Research Letters 33, L11307. doi:10.1029/2006GL026125.

Turmel, D., Locat, J., Cauchon-Voyer, G., Lavoie, C., Simpkin, P., Parker, G., Lauziere, P., 2010. Morphodynamic and slope instability observations at Wabush Lake, Labrador. In: Mosher, D.C., Craig Shipp, R., Moscardelli, L., Chaytor, J.D., Baxter, C.D.P., Lee, H.J., Urgeles, R. (eds). Submarine mass-movements and their consequences. Advances in Natural and Technological Hazards Research 28, pp. 435 – 446.

Van Daele, M., Moernaut, J., Doom, L., Boes, E., Fontijn, K., Heirman, K., Vandoorne, W., Hebbeln, D., Pino, M., Urrutia, R., Brümmer, R., De Batist, M., 2015. A comparison of the sedimentary records of the 1960 and 2010 great Chilean earthquakes in 17 lakes:

Implications for quantitative lacustrine palaeoseismology. Sedimentology 62, 1466-1496.

Villarosa, G., Outes, V., Gómez, E. A., Chapron, E., Ariztegui, D., 2009. Origen del tsunami de mayo de 1960 en el lago Nahuel Huapi, Patagonia: aplicación de técnicas batimétricas y sísmicas de alta resolución. Revista de la Asociación Geológica Argentina 65 (3), 593 – 597.

Volland, S., Sturm, M., Lukas, S., Pino, M., Müller, J., 2007. Geomorphological and sedimentological evolution of a lake basin under strong volcano-tectonic influence: The seismic record of Lago Calafquén (south-central Chile). Quaternary International 161, 32 – 45.

Waldmann, N., Anselmetti, F.S., Ariztegui, D., Austin Jr., J.A., Pirouz, M., Moy, C.M., Dunbar, R., 2011. Holocene mass-wasting events in Lago Fagnano, Tierra del Fuego (54°S): Implications for paleoseismicity of the Magallanes-Fagnano transform fault. Basin Research 23(2), 171-190.

Watt, S.F.L, Pyle, D.M., Naranjo, J.A., Mather, T.A., 2009. Landslide and tsunami hazard at Yate volcano, Chile, as an example of edifice destruction on strike-slip fault zones. Bulletin of Volcanology 71, 559 – 574.

Wirth, S.B., Girardclos, S., Rellstab, C., Anselmetti, F.S., 2011. The sedimentary response to a pioneer geo-engineering project: Tracking the Kander River deviation in the sediments of Lake Thun (Switzerland). Sedimentology 58 (7), 1737 – 1761.

Xue, Q., Zhang, M., Zhu, L., Cheng, X., Pei, Y., Bi, J., 2014. Quantitative deformation analysis of landslides based on multi-period DEM data. In: Kyoji S., Canuti, P., Yin, Y., (eds.). Landslide Science for a Safer Geo-Environment. Volume 2: Methods of Landslide Studies. Springer, Switzerland. pp 201-207.

Zaniboni, F., Armigliato, A., Pagnoni, G., Tinti, S., 2014. Continental margins as a source of tsunami hazard: The 1977 Gioia Tauro (Italy) landslide tsunami investigated through numerical modeling. Marine Geology 357, 210 – 217.

TABLE 1

TABLE 1: Morphometrical parameters estimated upon selected landslides. (T= translational motion; RT= combined rotational-translational motion; SP= slip plane; AA= undisturbed adjacent area; LS= lateral scarp; HS= headscarp

	Type	Area (m2)	Depth HS(m)	Length HS(m)	Height HS(m)	Slope (º) HS	Slope (º) LS W	Slope (º) LS E	Slope (º) AA	Slope (º) SP	Depleted volume (m3)	Accummulated volume (m3)	Run-out length (m)
Bar1	T	29233	64	175	3	25	12	8	17	18	77686	1711	≥1000
Cas1	RT	9643	9	91	6	36	15	18	21	24	15552	394	
Nire1	RT	135780	11	70	12	26	11	15	25	13	151118	77528	
Nire2	RT	156845	9	307	12	27	15	16	25	14	462352	12787	≥1700
Niri1	RT	121472	9	98	11	17	6	11	18	11	326680	660	
Niri2	RT	184563	11	257	8	22	15	14	14	7	413797	32451	

FIGURE CAPTIONS

Fig. 1. Map of the study area showing the fluvial catchments of the main inflowing streams and the active volcanoes affecting Lago Nahuel Huapi area. DNiri, DNire, DCas and DGut are Ñirihuau, Ñireco, Castilla and Gutierrez deltas, respectively. SCB=San Carlos de Bariloche; VLA=Villa La Angostura; DH=Dina Huapi; PSC= Puerto San Carlos.

Fig. 2. Subaqueous landsliding at the distal basin of Lago Nahuel Huapi. The morphometric analysis (Table 1) was performed upon the events indicated in white.

Fig. 3. Slope maps, 3D views and subtraction of the original ground surface (OGS) from the post-landslide surface (PLS) at (1) Bar1 and (2) Cas1. Black and blue lines indicate landslide scarps and subaqueous channels, respectively. Vertical exaggeration = 2x (3D view Cas1), 3x (3D view Bar1). Contour interval= 2 m. The red arrow in A) points out the structural lineament identified in the bathymetry.

Fig 4. Longitudinal (A) and transverse (B) seismic profiles across Bar 1. The failure initiated at the upper part of the slope that is coincident with a structural lineament (black dotted line). WLS=western lateral scarp; ELS=eastern lateral scarp. The grey dotted line indicates the area covered by the bathymetric survey.

Fig. 5. Slope maps, 3D views and subtraction of the original ground surface (OGS) from the post-landslide surface (PLS) at (1) Niri1 and (2) Niri2. Black and blue lines indicate landslide scarps and subaqueous channels, respectively. Grey circles show the areas possibly reworked by bottom or turbidity currents. U= unmobilized. Vertical exaggeration of the 3D views= 2x. Contour intervals= 2 m (PLS-OGS maps) and 5 m (Slope maps).

Fig. 6. Slope map, 3D views and subtraction of the original ground surface (OGS) from the post-landslide surface (PLS) at (1) Nire1 and (2) Nire2. Black lines indicate landslide scarps. Grey circles show the areas possibly reworked by bottom or turbidity currents. Vertical exaggeration of the 3D views= 2x. Contour interval= 2 m.

Fig. 7. Longitudinal (A) and transverse (B) seismic sections surveyed on May 2014 across key features of Nire2. The transverse section registered at the upper delta slope illustrate the proximity between adjacent landslides (L). The black rectangle indicates the location of Nire2. Undisturbed sediments (U) in the inner part of Nire2 show the unstratified alluvium observed in A). The grey dotted line in A) indicates the area covered by the bathymetric survey.

TABLE 1: Morphometrical parameters estimated upon selected landslides (T= translational motion; RT= combined rotational-translational motion; SP= slip plane; AA= undisturbed adjacent area; LS= lateral scarp; HS= headscarp

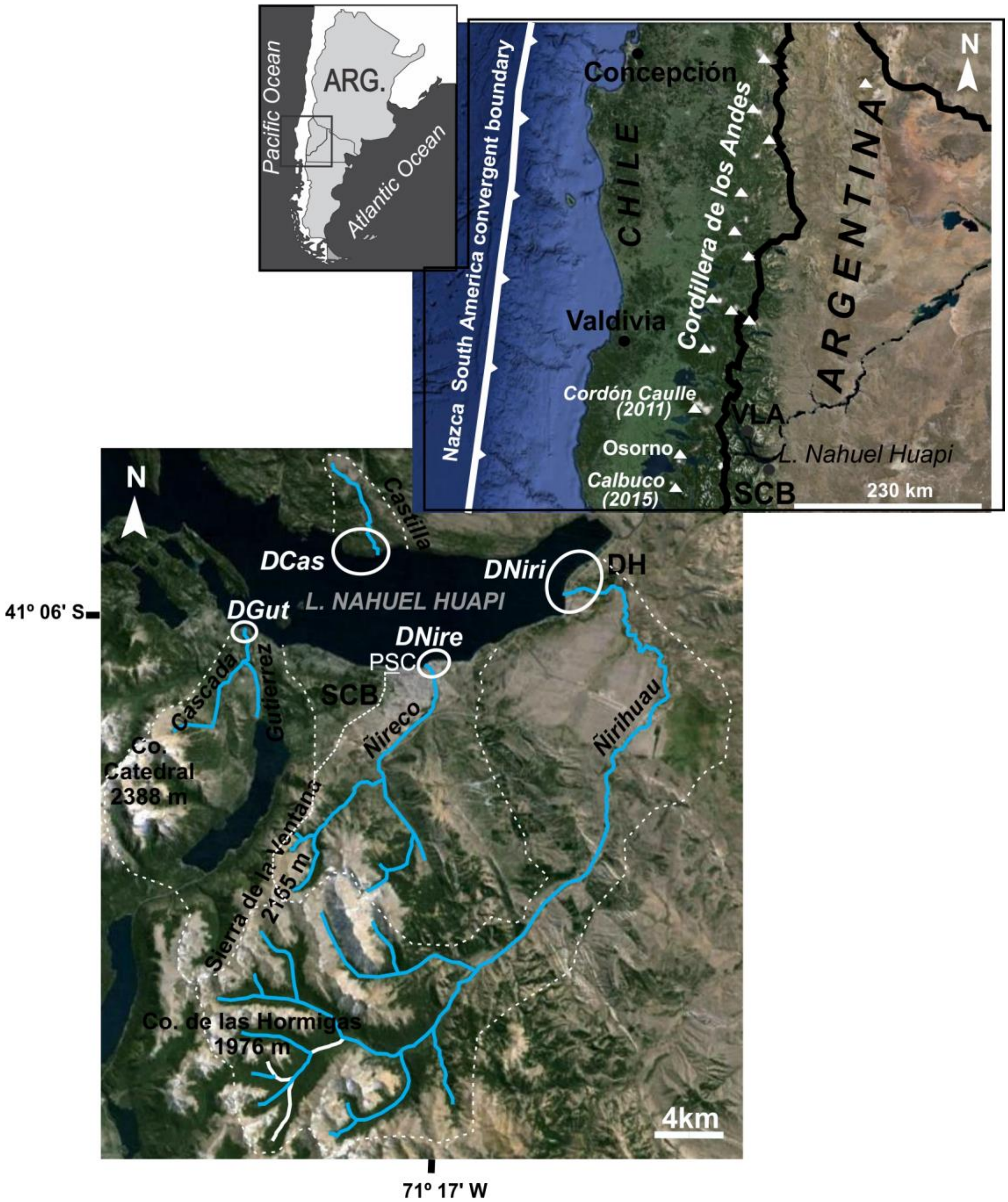
Pacific Ocean
ARG.
Atlantic Ocean
N
Nazca
South America convergent boundary
Concepción
CHILE
Cordillera de los Andes
ARGENTINA
Valdivia
Cordón Caulle (2011)
Osorno
Calbuco (2015)
VLA
L. Nahuel Huapi
SCB
230 km
N
DCas
Castilla
DNiri
DH
L. NAHUEL HUAPI
DGut
DNire
PSC
SCB
Cascada
Gutiérrez
Ñireco
Ñirihuau
Co. Catedral 2388 m
Sierra de la Ventana 2165 m
Co. de las Hormigas 1976 m
4km
41º 06' S
71º 17' W

Figure 1

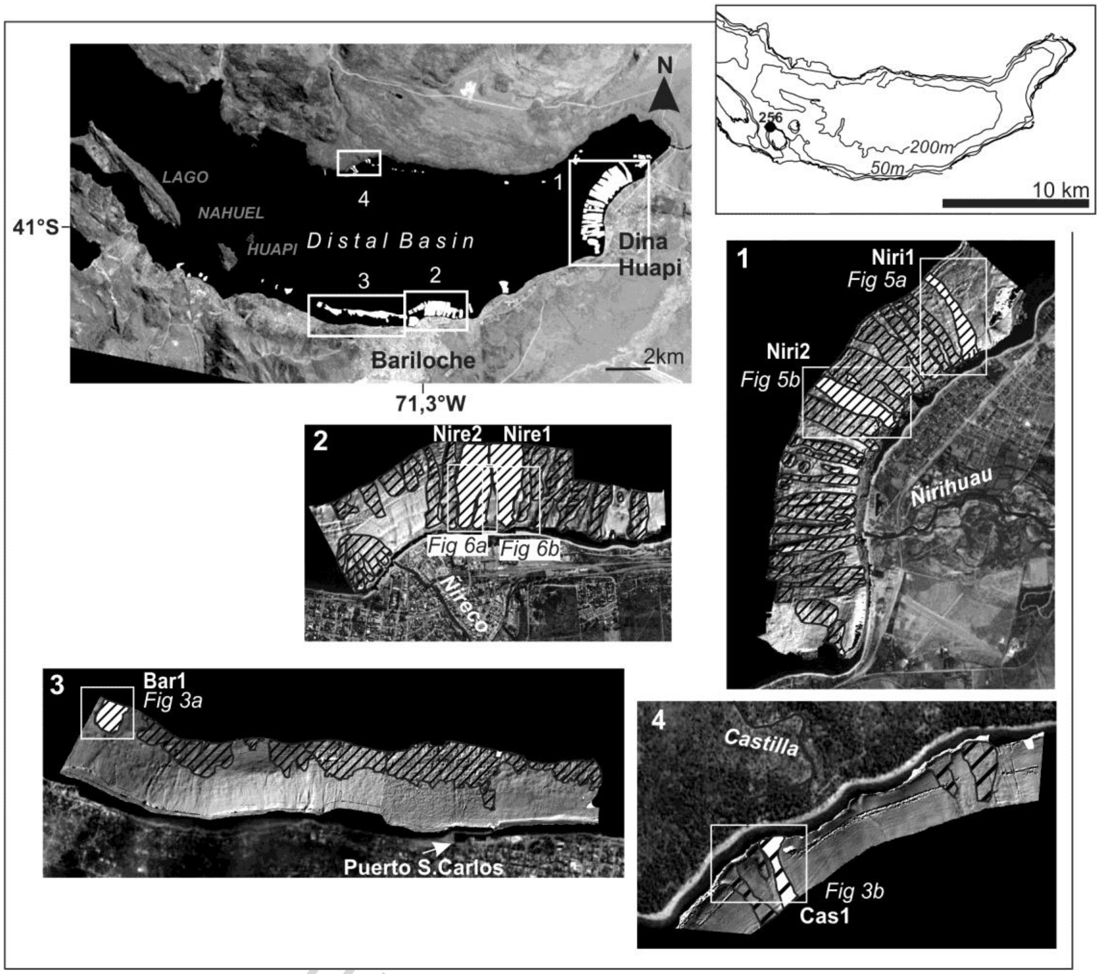
N
LAGO
NAHUEL
HUAPI
Distal Basin
41°S
1
2
3
4
Dina Huapi
Bariloche
71,3°W
2km
256
200m
50m
10 km
1
Niri1
Fig 5a
Niri2
Fig 5b
Nirihuau
2
Nire2
Nire1
Fig 6a
Fig 6b
Ñireco
3
Bar1
Fig 3a
Puerto S.Carlos
4
Castilla
Fig 3b
Cas1

Figure 2

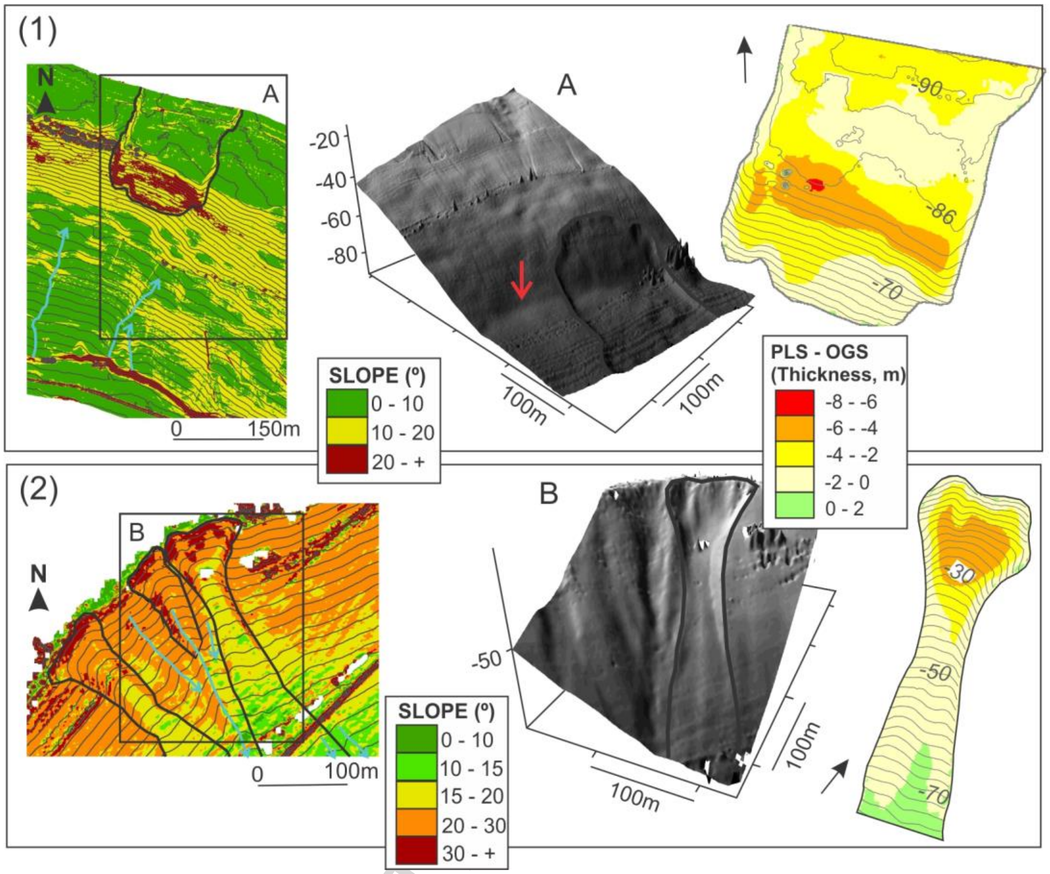
(1)
N
A
SLOPE (º)
0 - 10
10 - 20
20 - +
0
150m
-20
-40
-60
-80
100m
100m
-90
-86
-70
PLS - OGS
(Thickness, m)
-8 - -6
-6 - -4
-4 - -2
-2 - 0
0 - 2
(2)
B
N
-50
100m
100m
-30
-50
-70
SLOPE (º)
0 - 10
10 - 15
15 - 20
20 - 30
30 - +
0
100m

Figure 3

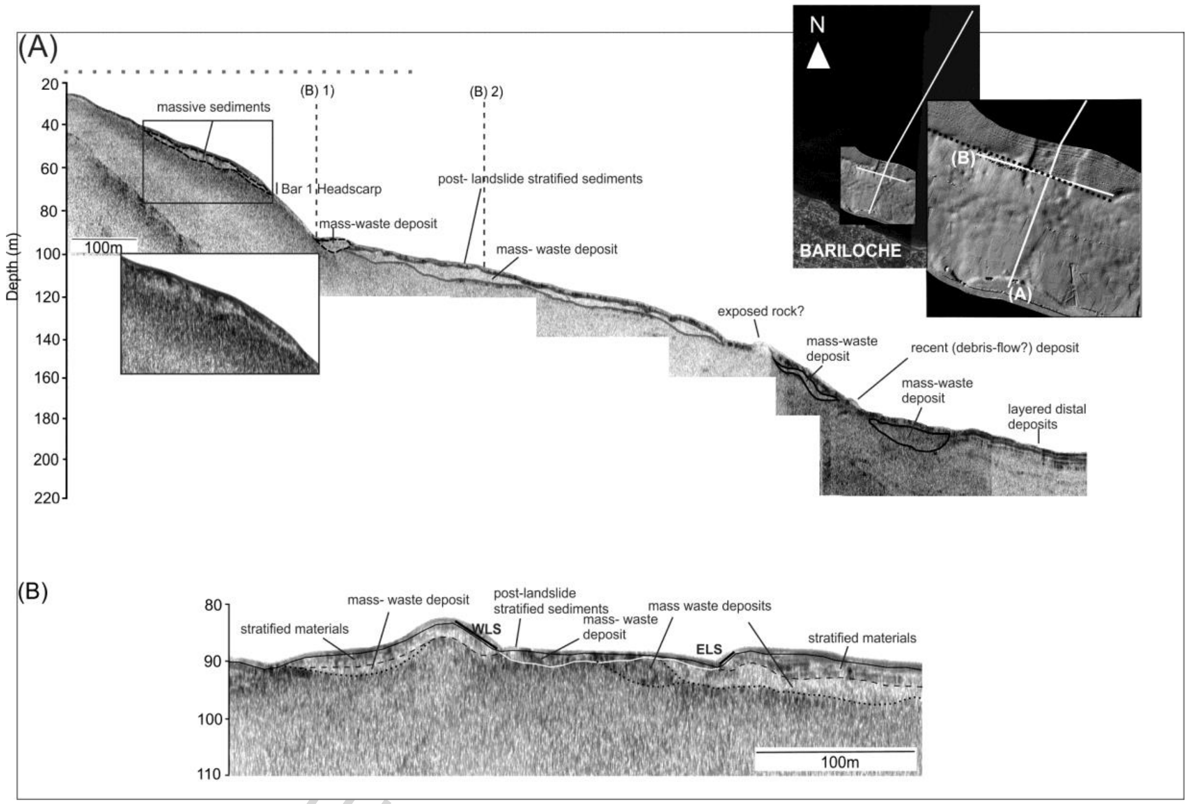
(A)
20
40
60
80
100
120
140
160
180
200
220
Depth (m)
100m
massive sediments
Bar 1 Headscarp
(B) 1)
(B) 2)
mass-waste deposit
post- landslide stratified sediments
mass- waste deposit
exposed rock?
mass-waste deposit
recent (debris-flow?) deposit
mass-waste deposit
layered distal deposits
N
BARILOCHE
(B)
(A)
(B)
80
90
100
110
stratified materials
mass- waste deposit
post-landslide stratified sediments
WLS
mass- waste deposit
mass waste deposits
ELS
stratified materials
100m

Figure 4

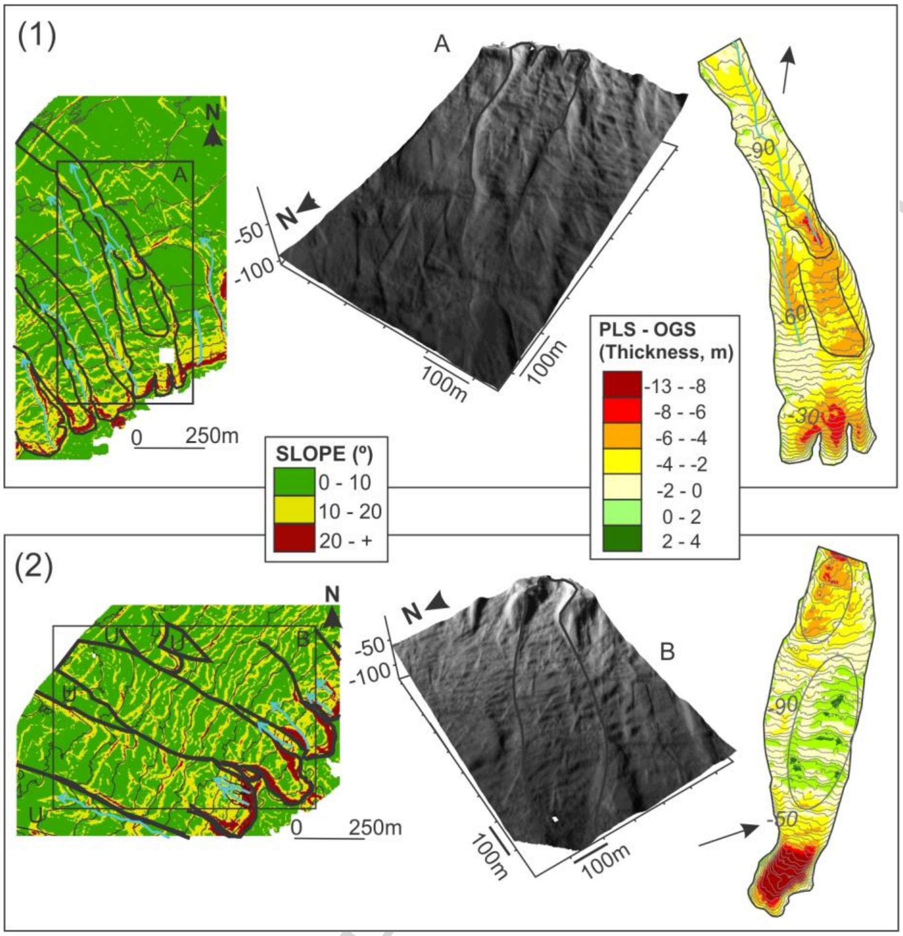

(1)
A
N
250m
0
-50
-100
100m
100m
90
60
30
SLOPE (º)
0 - 10
10 - 20
20 - +
PLS - OGS
(Thickness, m)
-13 - -8
-8 - -6
-6 - -4
-4 - -2
-2 - 0
0 - 2
2 - 4
(2)
B
-50
-100
100m
100m
90
50

Figure 5

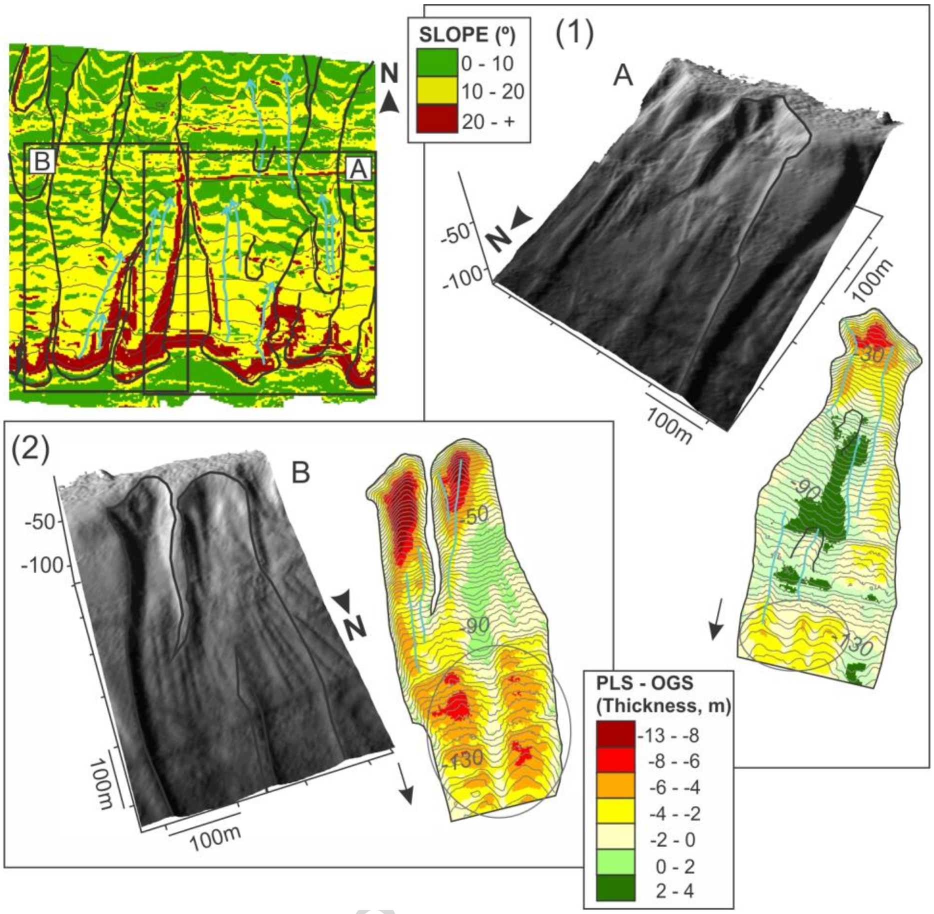

SLOPE (º)
0 - 10
10 - 20
20 - +
N
B
A
(1)
A
-50
-100
N
100m
100m
-30
-90
-130
(2)
B
-50
-100
N
100m
100m
-50
90
-130
PLS - OGS
(Thickness, m)
-13 - -8
-8 - -6
-6 - -4
-4 - -2
-2 - 0
0 - 2
2 - 4

Figure 6

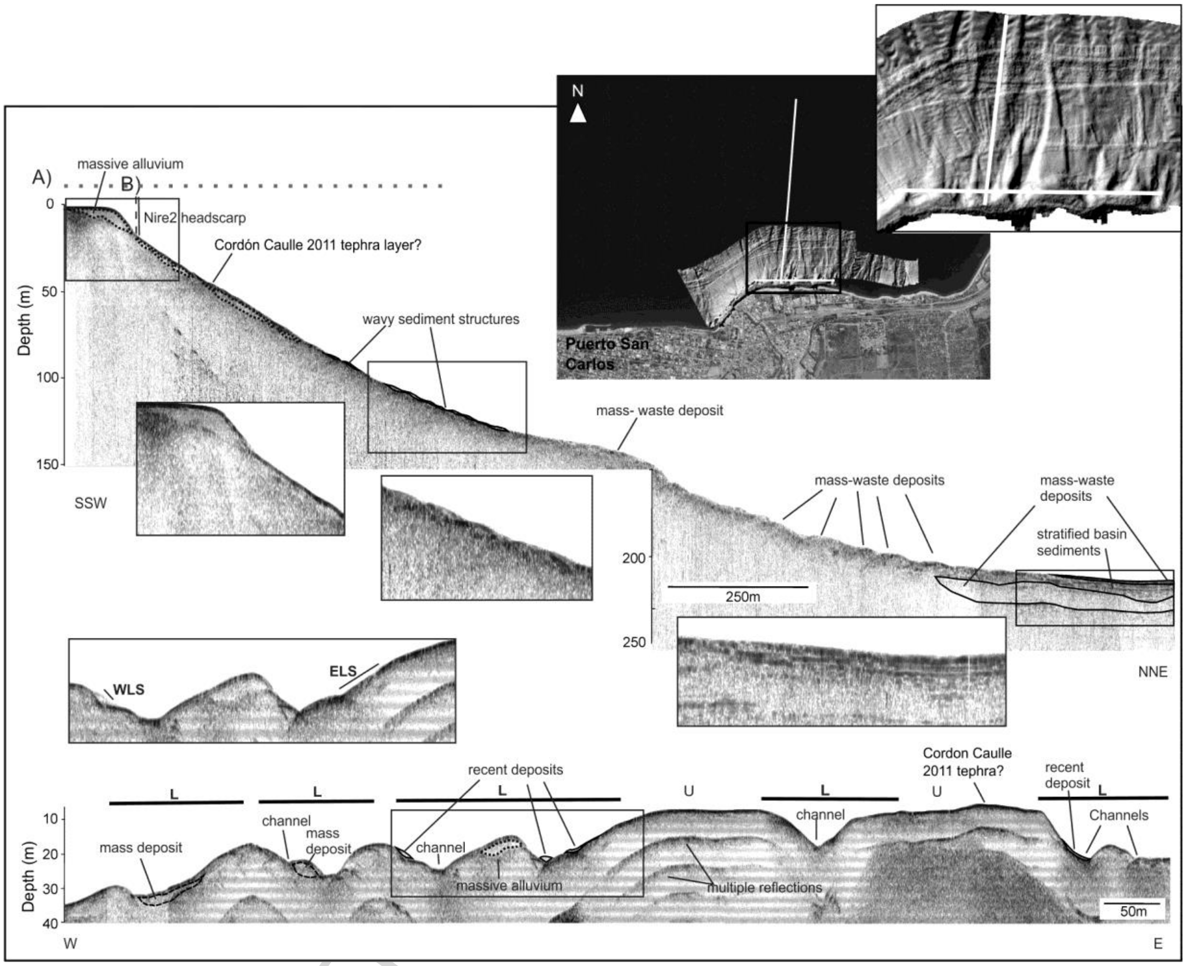

N
Puerto San Carlos
A)
B)
massive alluvium
Nire2 headscarp
Cordón Caulle 2011 tephra layer?
Depth (m)
0
50
100
150
200
250
wavy sediment structures
mass- waste deposit
mass-waste deposits
mass-waste deposits
stratified basin sediments
250m
SSW
NNE
WLS
ELS
L
U
recent deposits
Cordon Caulle 2011 tephra?
recent deposit
channel
mass deposit
Channels
massive alluvium
multiple reflections
10
20
30
40
50m
W
E

Figure 7

Highlights

- Subaqueous mass-wasting features and sediment waves were studied in a Patagonian lake
- Landslide inventory and morphometric analysis of mass wasting bedforms are presented
- Urbanized lacustrine deltas are landslide-prone environments
- Mobilization, transport and sedimentation of subaqueous deposits are discussed